nature structural & molecular biology

Substrate binding on the APC/C occurs between the coactivator Cdh1 and the processivity factor Doc1

Bettina A Buschhorn[1,5], Georg Petzold[1,5], Marta Galova[1], Prakash Dube[2], Claudine Kraft[1,4], Franz Herzog[1,4], Holger Stark[2,3] & Jan-Michael Peters[1]

The anaphase-promoting complex/cyclosome (APC/C) is a 22S ubiquitin ligase complex that initiates chromosome segregation and mitotic exit. We have used biochemical and electron microscopic analyses of *Saccharomyces cerevisiae* and human APC/C to address how the APC/C subunit Doc1 contributes to recruitment and processive ubiquitylation of APC/C substrates, and to understand how APC/C monomers interact to form a 36S dimeric form. We show that Doc1 interacts with Cdc27, Cdc16 and Apc1 and is located in the vicinity of the cullin–RING module Apc2–Apc11 in the inner cavity of the APC/C. Substrate proteins also bind in the inner cavity, in close proximity to Doc1 and the coactivator Cdh1, and induce conformational changes in Apc2–Apc11. Our results suggest that substrates are recruited to the APC/C by binding to a bipartite substrate receptor composed of a coactivator protein and Doc1.

Sister chromatid separation and exit from mitosis are initiated by a 1.5-MDa ubiquitin ligase (E3) composed of at least 13 subunits and known as the anaphase-promoting complex/cyclosome (APC/C)[1]. The APC/C initiates these events by ubiquitylating substrate proteins such as securin and cyclin B, which are subsequently degraded by the 26S proteasome. Recognition of substrates by the APC/C depends on coactivator proteins, called Cdc20 and Cdh1, which promote substrate recruitment by interacting both with the APC/C and with recognition motifs in the substrates known as the destruction box (D box) and KEN box. The subsequent ubiquitylation of substrates is mediated by ubiquitin-conjugating (E2) enzymes that interact with a RING-finger subunit of the APC/C, called Apc11 (ref. 2). Before all chromosomes have been bioriented on the mitotic spindle, the spindle-assembly checkpoint (SAC) inhibits the form of the APC/C that is interacting with Cdc20 (APC/C^{Cdc20}) by promoting assembly of a mitotic checkpoint complex (MCC) in which Mad2, BubR1 and Bub3 bind to Cdc20 (APC/C^{MCC})[3].

Structural information will be essential to understanding the mechanism of APC/C-mediated ubiquitylation reactions, but so far, only crystal structures of the 35-kDa APC/C subunit Doc1 (also known as Apc10; refs. 4,5) and of parts of the tetratricopeptide repeat (TPR) subunits Cdc16, Cdc27 and Apc7 have been solved[6–8]. Therefore, electron microscopy (EM) has been used to analyze the structure of the APC/C. For human[9,10], *Xenopus laevis*[9] and fission yeast APC/C[11], this has revealed that the APC/C complex has a roughly triangular shape and is largely composed of two domains, called the "platform" and the "arc lamp," that together enclose a central cavity (see discussion below), whereas a model obtained for budding yeast (*S. cerevisiae*) APC/C shows a more globular structure[12]. Biochemical and EM subunit mapping experiments in different species[9–11,13–15] have indicated that the platform domain contains Apc1, Apc4 and Apc5, whereas the arc lamp domain consists of the TPR proteins Cdc16, Cdc23, Cdc27 and, in case of the vertebrate APC/C, presumably also Apc7. Apc2, a member of the cullin protein family, is located between the platform and the "head" of the arc lamp domain, whereas Cdc20 and Cdh1 bind to the arc lamp opposite Apc2, with Apc2 and coactivators both facing the central cavity.

Because Apc2's interaction partner Apc11 interacts with E2 enzymes and coactivator proteins help to recruit substrates, it has been speculated that ubiquitylation reactions occur in the inner cavity[9,10]. However, direct evidence for substrate recruitment to this site is so far lacking. Also unknown is the location of Doc1, a subunit that has been implicated in substrate binding to the APC/C[16] and in processive substrate ubiquitylation[17]. How Doc1 contributes to these processes is unknown, but the protein is structurally similar to ligand-binding domains in bacterial sialidases and some other enzymes[4,5], and related "Doc domains" are also found in other ubiquitin ligases[18,19]. It is therefore possible that Doc1 uses its putative ligand-binding region to interact with APC/C substrates. Consistent with this hypothesis, Doc1's ligand-binding domain is required for its ability to confer processivity to the APC/C[20]. However, direct evidence for Doc1-substrate interactions has not been obtained.

Here we have used biochemical reconstitution experiments to isolate various forms of budding yeast and human APC/C and have

[1]Research Institute of Molecular Pathology (IMP), Vienna, Austria. [2]Max Planck Institute for Biophysical Chemistry, Göttingen, Germany. [3]Department of Molecular 3D Electron Cryomicroscopy, Institute of Microbiology and Genetics, Georg-August Universität Göttingen, Göttingen, Germany. [4]Present addresses: Institute of Biochemistry, Eidgenössische Technische Hochschule Zürich, Zürich, Switzerland (C.K.); Institute of Molecular Systems Biology, Eidgenössische Technische Hochschule Zürich, Zürich, Switzerland (F.H.). [5]These authors contributed equally to this work. Correspondence should be addressed to H.S. (hstark1@gwdg.de) or J.-M.P. (peters@imp.ac.at).

Received 27 July; accepted 17 November; published online 26 December 2010; doi:10.1038/nsmb.1979

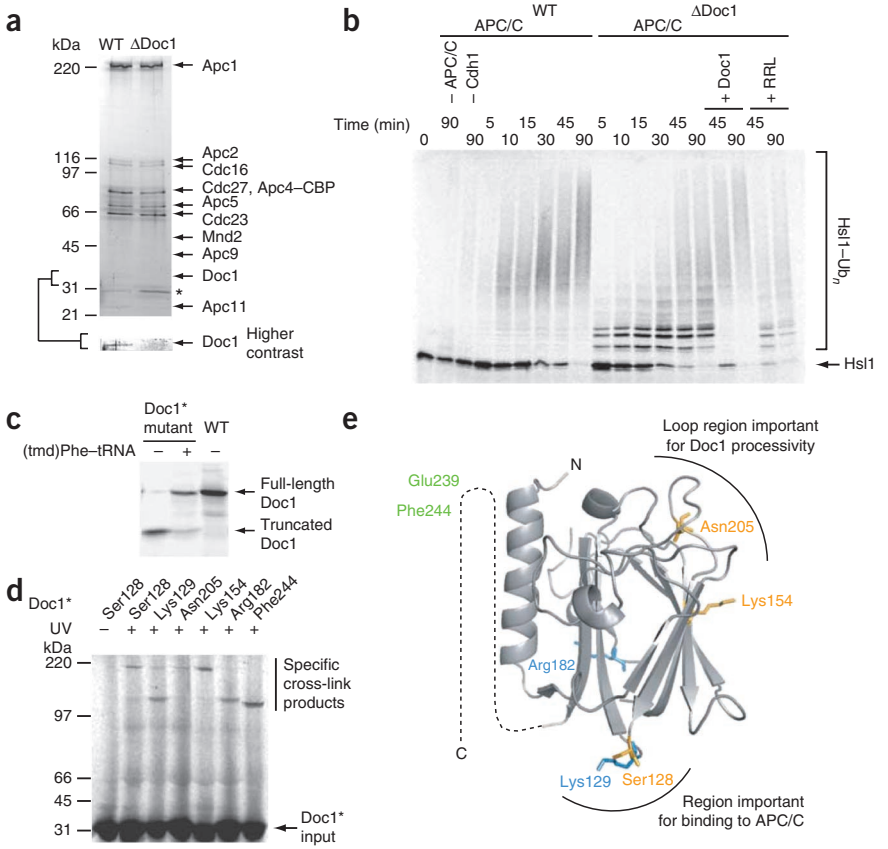

Figure 1 Incorporation of a photo-cross-linker into Doc1 results in cross-link products between Doc1 and APC/C subunits. (**a**) Composition of wild-type APC/C (WT) and APC/C lacking Doc1 (ΔDoc1) affinity-purified via a TAP tag on Apc4. Apc4–CBP indicates calmodulin-binding protein that remains on Apc4 after TEV cleavage. Asterisk marks contaminating band. (**b**) APC/C ubiquitylation of [^{35}S]methionine-labeled Hsl1$_{667–872}$ substrate is impaired when Doc1 is absent as compared to when the wild-type form of APC/C is present. (**c**) Cross-linker incorporation into *in vitro*–translated Doc1. Full-length Doc1 contains the photoactivatable amino acid. (**d**) Overview of cross-link products obtained with ^{35}S-labeled Doc1 amber mutants carrying the photo-cross-linker at six different sites. The two consecutive sites Ser128 and Lys129 each created two cross-link products of different sizes. (**e**) Doc1 crystal structure of *S. cerevisiae*. Cross-linker incorporation sites are indicated. Predominant cross-links of APC/C subunits to respective Doc1 sites are color coded (green, Cdc27; blue, Cdc16, orange, Apc1).

analyzed these complexes by using photo-cross-linking, single-particle EM and three-dimensional (3D) reconstruction. Our results show that the structure of the APC/C is conserved from budding yeast to vertebrates and that Doc1 is located in close vicinity to the cullin–RING module Apc2–Apc11. Structural analysis of human APC/C^{CDH1}–substrate complexes revealed that the substrate density is found in the inner cavity, directly intercalated between CDH1 and DOC1. These observations suggest that CDH1 and DOC1 form a bipartite substrate receptor on the APC/C.

RESULTS

Doc1 cross-links to Cdc27, Cdc16 and Apc1 in yeast APC/C

To understand how Doc1 interacts with the APC/C, we generated radiolabeled forms of Doc1 containing a photoactivatable cross-linker at defined sites, allowed these Doc1 proteins to bind to APC/C lacking endogenous Doc1 and used photo-cross-linking followed by SDS-PAGE and phosphorimaging to identify cross-link products between Doc1 and APC/C subunits. We used APC/C from budding yeast for these experiments because previous work had shown that APC/C can be purified from yeast strains from which the *DOC1* gene has been deleted and because the processivity defect of the resulting APC/C$^{\Delta Doc1}$ complexes can be restored *in vitro* by addition of recombinant Doc1 (refs. 16,20). Earlier studies used a version of Doc1 containing 283 amino acid residues[20,21], whereas the *Saccharomyces* genome database (SGD; http://www.yeastgenome.org/) reports only 250 residues for Doc1 (lacking 38 residues at the N terminus). Because we could identify only the latter form of Doc1 associated with endogenous APC/C (**Supplementary Fig. 1a**), we used a cDNA that encodes the 250-residue version of Doc1. When this form of Doc1 was synthesized by coupled *in vitro* transcription-translation in rabbit reticulocyte lysate and added to purified APC/C$^{\Delta Doc1}$ in the presence of the ubiquitin-activating enzyme E1, the E2 enzyme Ubc4, Cdh1 and a fragment of the APC/C substrate Hsl1 (Hsl1$_{667–872}$), Doc1 restored the ability of APC/C$^{\Delta Doc1}$ to generate high-molecular-weight Hsl1–ubiquitin conjugates (**Fig. 1a**,**b** and **Supplementary Fig. 1b**), indicating that the short form of Doc1 used here is functional.

To generate forms of Doc1 that contain cross-linkers, we introduced amber (TAG) stop codons into different sites in the coding sequence of the Doc1 cDNA. We used the resulting mutated cDNAs as templates in *in vitro* transcription-translation reactions that contained [^{35}S]methionine, [^{35}S]cysteine and an amber suppressor tRNA coupled to the artificial amino acid L-4′-(3-[trifluoromethyl]-3*H*-diazirine-3-yl)phenylalanine (hereafter called (tmd)Phe[22]). Use of the suppressor tRNA allowed translation beyond the amber stop codon, resulting in ^{35}S-labeled Doc1 carrying (tmd)Phe at the sites specified by the amber codon (**Fig. 1c**). We inserted (tmd)Phe at any one of 24 different positions, representing nearly 10% of all residues in Doc1 (**Supplementary Table 1**). When incubated with APC/C$^{\Delta Doc1}$, 7 of the 24 Doc1 mutants reproducibly yielded cross-link products with molecular masses of 120 kDa (Phe224amber, Glu239amber), 140 kDa (Lys129amber, Arg182amber) and 200 kDa (Ser128amber, Lys154amber, Asn205amber; **Fig. 1d** and **Supplementary Table 2**). **Figure 1e** shows positions in the Doc1 structure at which (tmd)Phe was inserted in these mutants.

All cross-link products were obtained only in the presence of APC/C (see **Fig. 2** and data not shown), indicating that these products represented Doc1 that was cross-linked to APC/C subunits. To determine the identity of these subunits, we fused all APC/C subunits whose molecular mass was consistent with them being part of the Doc1 cross-link products (Apc1, Apc2, Cdc27, Cdc16 and Apc5) to myc6, myc9 or myc18 tags, which are known to reduce protein electrophoretic mobility[23]. These experiments identified cross-link products formed between Doc1 and three different APC/C subunits (**Fig. 2a–c** and **Supplementary Table 2**): Doc1-Phe244amber yielded cross-link products with Cdc27, consistent with the observation that the very C-terminal portion of Doc1, in which Phe244 (and also Glu239) is located, is required for Cdc27 binding *in vitro*[5]. Doc1-Ser128amber

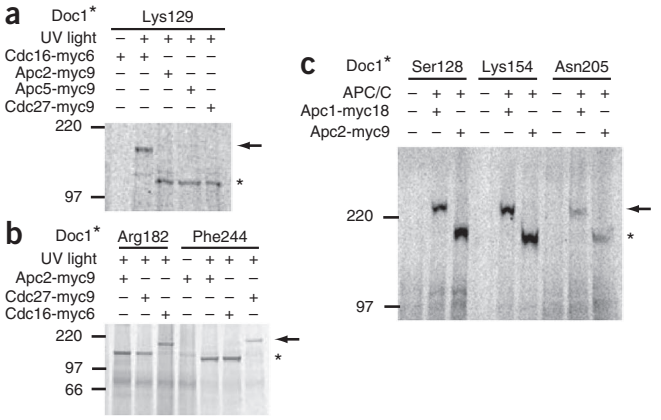

Figure 2 Identification of APC/C subunits that interact with Doc1. (**a**) Cdc16-myc6 incorporated into the APC/C complex caused a mobility shift of the cross-link product (arrow) when incubated with radiolabeled Doc1 carrying the photo-cross-linker at the position of Lys129, which indicates an interaction between Doc1-Lys129 and Cdc16. (**b**) Doc1 residue Arg182 contacts Cdc16. Cdc27 interacts with Doc1 via residue Phe244. (**c**) The large subunit Apc1 contacts the Doc1 protein at residues Ser128, Lys154 and Asn205. Arrows indicate the mobility shift of the cross-link product (asterisk).

and Doc1-Lys129amber, which are located in the C-terminal region of Doc1, and Doc1-Arg182amber, located on the back side of Doc1, formed cross-link products with Cdc16. Two Doc1 mutants, Doc1-Ser128amber and Doc1-Lys154amber, predominantly formed cross-link products with Apc1, but less abundant Apc1 cross-link products were also obtained with Doc1-Lys129amber and Doc1-Asn205amber (note that Doc1-Ser128amber predominantly formed cross-link products with Apc1 but also did so less frequently with Cdc16, whereas Doc1-Lys129amber showed the opposite behavior, forming cross-link products preferentially with Cdc16 but also to a lesser degree with Apc1; for possible interpretations of this result, see Discussion). Doc1-Glu239amber was not analyzed because Doc1-Glu239amber and Doc1-Phe244amber yielded indistinguishable cross-link products, suggesting that they both interact with the same APC/C subunit (Cdc27). These results suggest that Doc1 interacts with the APC/C by contacting at least three other subunits, Cdc27, Cdc16 and Apc1.

Localization of Doc1 in budding yeast and human APC/C

To better understand Doc1's interactions with other APC/C subunits, we identified the position of Doc1 within the structure of APC/C. Because the previously reported 3D model of budding yeast APC/C[12] differed substantially from the structures obtained for human and

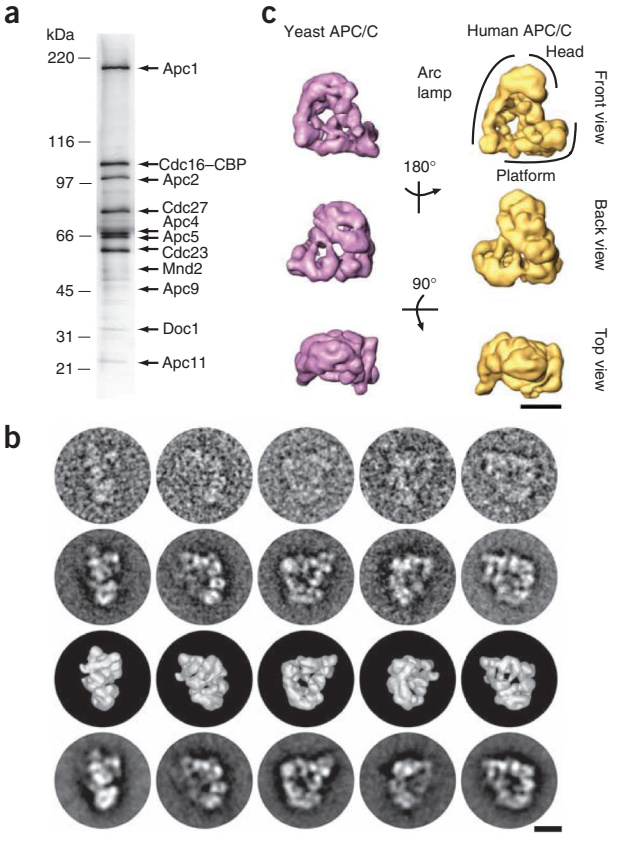

Xenopus APC/C[9,10], we first determined a 3D structure of yeast APC/C (**Fig. 3a**) at ~25-Å resolution by cryo-negative staining EM (**Fig. 3b**,**c** and **Supplementary Table 3**). This structure revealed that yeast APC/C, like vertebrate APC/C, is composed of a platform and an arc lamp domain that together enclose a central cavity. The dimensions of the platform domain are similar in yeast, *Xenopus* and human APC/C (135 × 130 Å in yeast APC/C), but the arc lamp domain of yeast APC/C is shorter than the corresponding domain in vertebrate APC/C (195 Å high in yeast *versus* 230 Å in human APC/C). Otherwise, the structures of yeast and vertebrate APC/C are similar in shape and size, indicating that APC/C's structure has been largely conserved during evolution.

We identified the location of Doc1 within the APC/C by using three different approaches (**Fig. 4**). First, comparison of the 3D structure of wild-type yeast APC/C with a structure obtained for APC/C$^{\Delta Doc1}$ revealed that a small density located on top of the inner cavity and under the head of the arc lamp domain was absent in APC/C$^{\Delta Doc1}$ (**Fig. 4a**). Second, we generated a strain in which the N terminus of Doc1 was fused to a 56-kDa tag called tdimer2 (td2), which is composed of two copies of the red fluorescent protein DsRed[24,25] (**Supplementary Fig. 1c**). When APC/C containing only this version of Doc1 was analyzed by EM and 3D reconstruction, an extra density was observed next to the density that was absent in the structure of APC/C$^{\Delta Doc1}$ (**Fig. 4a**,**b**). This observation supports the notion that the density identified by difference mapping between wild-type APC/C and APC/C$^{\Delta Doc1}$ represents the position of the Doc1 protein. Third, we used antibodies to human DOC1 to map the location of this subunit in human APC/C. We incubated APC/C purified from HeLa cells with DOC1 antibodies at an APC/C-to-antibody ratio that led to the formation of trimers in which two APC/C particles were bound by one IgG molecule, enriched these complexes by glycerol density-gradient

Figure 3 Purification and 3D reconstruction of budding yeast APC/C. (**a**) SDS-PAGE of APC/C TAP tag purified via Cdc16. APC/C subunits were identified from their characteristic electrophoretic mobility and by MS. (**b**) EM analysis of yeast APC/C. Top row shows selected EM raw images of yeast APC/C in different orientations. Class averages were obtained by alignment, multivariate statistical analysis and classification of the raw images and are shown in the second row. The third row shows the surface representation of the computed yeast APC/C 3D structure in the corresponding orientations. The fourth row shows re-projections of the yeast APC/C 3D structure in angular directions determined for the views in the third row. (**c**) Surface representations of yeast and human APC/C 3D structures in three different orientations. Indicated rotations refer to the top structures. The location of APC/C's head, arc lamp and platform domain is indicated. Size bars, 10 nm.

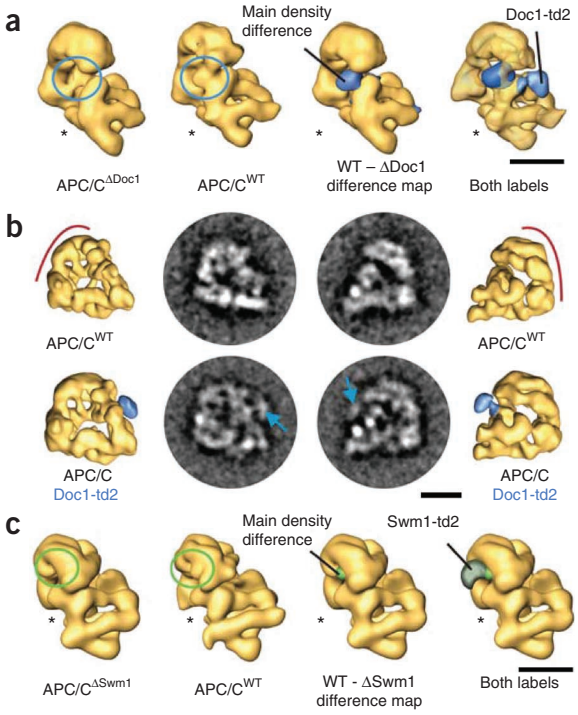

Figure 4 Localization of Doc1 and Swm1 in the yeast APC/C 3D structure by subunit deletion and td2 labeling. (**a**) 3D models illustrating Doc1 localization. Density not present in APC/C$^{\Delta Doc1}$ compared to APC/C^{WT} is labeled as main density difference in the APC/C WT – ΔDoc1 difference map. Subunit deletion and td2 labeling converge at identical locations. (**b**) Labeling and EM analysis of td2-Doc1 compared to wild-type APC/C. Class averages of wild-type and Doc1-td2–labeled APC/C are shown in two different orientations. The additional density caused by the td2 tag is indicated with arrows in the class averages. 3D models computed from the corresponding datasets are depicted in similar orientations. (**c**) Localization of Swm1 using subunit deletion and td2 labeling. Swm1 is located in the head domain. The asterisks mark the face of APC/C's central cavity. Size bars, 10 nm.

centrifugation and used negative staining EM to determine the region on APC/C to which the DOC1 antibodies had been bound (**Supplementary Fig. 1d**,**e**). These experiments indicated that in the structure of human APC/C, as in that of yeast, DOC1 is located above the inner cavity and below the head of the arc lamp domain.

Localization of yeast APC/C subunits

To determine whether the position of Doc1 within the APC/C structure is consistent with the observation that Doc1 can form cross-link products with Cdc27, Cdc16 and Apc1, we mapped the location of these subunits in the 3D structure of yeast APC/C. We tagged Cdc27 and Cdc16 at their C termini with td2, and Apc1 with a tag that contained a single copy of DsRed (called "tm" for tmonomer; viable strains expressing Apc1-td2 could not be obtained). We purified APC/C containing Cdc27-td2, Cdc16-td2 or Apc1-tm and obtained 3D structures for these complexes (**Fig. 5** and **Supplementary Fig. 2**). These experiments revealed that Cdc27 is located in the "head" of the arc lamp domain and Cdc16 in a central region of the arc lamp domain, next to the putative location of Cdc27 (**Fig. 5b**,**c**): in other words, Cdc27 and Cdc16 are located above and behind Doc1. The tag fused to the C terminus of Apc1 protruded from the platform domain into the inner cavity of APC/C: that is, it was located below Doc1 (**Supplementary Fig. 2d**). Although it cannot be inferred from these data that Doc1 directly contacts Cdc27, Cdc16 and Apc1, the EM data are consistent with this possibility.

We also used the techniques developed for localization of Doc1 to identify the position of other APC/C subunits. In case of Swm1 (also called Apc13), one of the few APC/C subunits that are not essential for viability in yeast[14,16,26,27], we purified APC/C from a strain from which the *SWM1* gene had been deleted. In the APC/C$^{\Delta Swm1}$ structure, a small density was missing on the front side of the head of the arc lamp domain, next to Cdc16 and Cdc27 (**Figs. 4c** and **5c**). A 3D structure of APC/C in which Swm1 had been tagged with td2 revealed an extra globular density right next to the putative Swm1 density identified by difference mapping (**Fig. 4c**). Swm1 is therefore located in the vicinity of Cdc16 and Cdc27, consistent with the observation that Swm1 stabilizes interactions between these two subunits[14].

We attempted to use td2 tagging for the remaining APC/C subunits as well, but we were able to obtain viable yeast strains and APC/C samples suitable for EM only for Apc11 and Apc5. The resulting 3D structures revealed an additional globular domain in the central cavity, close to Doc1, when td2 had been fused to the C terminus of Apc11 (**Fig. 5c** and **Supplementary Fig. 2c**,**d**), consistent with the previously identified location of APC11's binding partner, APC2, in human APC/C[9,10]. C-terminal tagging of Apc5 with td2 revealed an extra density on the left side of the platform domain (**Fig. 5c** and **Supplementary Fig. 2b**,**d**), also consistent with the previous localization of APC5 in human APC/C[10].

EM analysis of dimeric forms of yeast APC/C

The majority of APC/C observed in our EM specimens was monomeric, but dimeric forms of APC/C were also present (**Supplementary Fig. 3a**), confirming previous reports[12,16]. As shown before[23], we found that APC/C sedimented corresponding to a sedimentation coefficient of 36S when yeast extracts were fractionated in the presence of low salt concentrations (50 mM KCl). However, when the same yeast extracts were analyzed in the presence of 400 mM KCl, most APC/C sedimented as a 22S particle (**Supplementary Fig. 3b**,**c**),

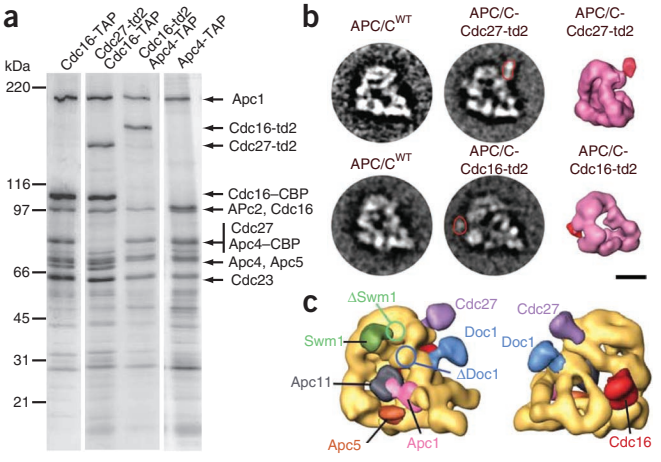

Figure 5 APC/C subunit localization using td2 labeling. (**a**) SDS-PAGE analysis of td2-labeled Cdc16 or Cdc27 subunits incorporated into yeast APC/C. (**b**) Class averages of APC/C-Cdc27-td2 and APC/C-Cdc16-td2 compared to wild-type APC/C. Extra densities caused by the td2 label are highlighted in the class averages and marked in red in the respective 3D models. Size bar, 10 nm. (**c**) Results of all labeling experiments carried out in this study superimposed onto the structure of yeast APC/C.

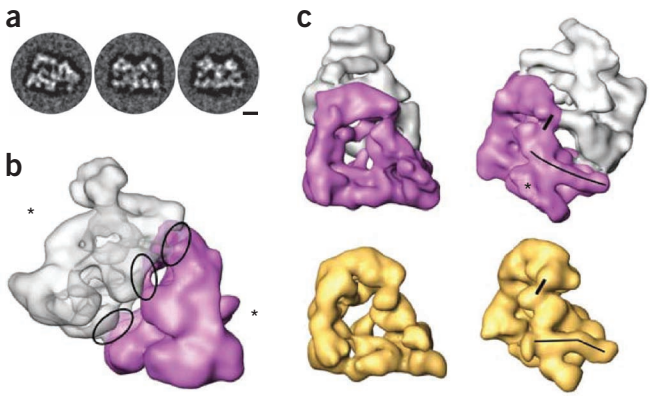

Figure 6 Analysis of APC/C dimers. (**a**) Class averages of dimeric APC/C with different orientations. Size bar, 10 nm. (**b**) 3D model of dimeric APC/C. The purple APC/C monomer is shown in a side view orientation with the TPR-rich arc lamp domain in the front. The gray APC/C monomer is shown in a bottom view orientation with the bottom of the platform domain in the front. Asterisks mark the face of APC/C's central cavity. The middle ellipse marks a unique contact lying on the *c*2 symmetry axis, whereas the other ellipses show contact points that each exist as an asymmetric pair. (**c**) APC/C dimerization causes conformational rearrangements in the platform domain as well as the head domain compared to monomeric APC/C (yellow). Black lines and asterisk indicate conformational changes between monomeric and dimeric APC/C.

as does purified monomeric yeast APC/C[28]. These observations indicate that many APC/C particles in yeast extracts exist as dimers that dissociate into monomers in the presence of buffers with high ionic strength. Because these findings are consistent with the possibility that yeast APC/C can also exist as a dimer *in vivo*, we also generated a 3D structure of dimeric APC/C at a resolution of ~35 Å. Images of these dimers could be sorted into class averages of similar orientations (**Fig. 6a**), indicating that these dimers represent a homogeneous population of particles in which two APC/C monomers adopt a defined orientation.

The resulting 3D structure revealed that APC/C monomers within the dimer interact via five discrete contact points (three of which can be seen in **Fig. 6b**, marked by ellipses), mostly on the back side of the arc lamp and the platform domains (**Fig. 6b**,**c**). One of these points lies on a *c*2 symmetry axis and is generated by a contact between the same regions of the arc lamp domain where Cdc27 is located and thus possibly through a homotypic interaction between two Cdc27 molecules. The other contacts are not located on the *c*2 axis and thus occur as asymmetrical pairs of interactions (subunit A of monomer 1 interacts with subunit B of monomer 2 and vice versa). The first pair of contacts is generated by interactions between Apc1 in the platform domain and an unidentified subunit located on the back side of the arc lamp domain, possibly Cdc27, Cdc16 or Cdc26. The second pair of contacts is formed between Cdc16 and an unidentified subunit on the back side of the platform, possibly Apc1 or Apc2.

During 3D reconstruction, we applied two-fold symmetry, which prevents the detection of differences in conformation between APC/C monomers within the dimer. However, the conformation of APC/C in the dimer is clearly different from the conformation of monomeric APC/C. Whereas Apc1 has a characteristic bent shape in monomeric APC/C, it adopts a straighter conformation in the dimer, pointing upward into the direction of Doc1 (the conformational change in Apc1 is indicated by long black lines in **Fig. 6c**). Smaller conformational changes could also be observed for densities that correspond to Apc4, Cdc27 and Doc1. In the monomer, the density of Apc4 is better defined and the contact between Cdc27 and Doc1 (indicated by short black lines in **Fig. 6c**) is more pronounced than in the dimer.

Because the dimeric form of yeast APC/C has been reported to ubiquitylate substrates with higher processivity than monomeric APC/C[12], we tested whether the role of Doc1 in APC/C processivity could be explained by a requirement for Doc1 in APC/C dimerization. When we analyzed proteins in whole cell extract from yeast Δ*doc1* strains, however, we observed that Cdc16 sedimented as a 36S particle, and in EM specimens of APC/C$^{\Delta Doc1}$, dimers could still be detected (data not shown), indicating that APC/C$^{\Delta Doc1}$ also exists in a dimeric form (see also **Supplementary Fig. 3d**). Doc1 therefore is not required for APC/C dimerization and must contribute to APC/C processivity through other mechanisms.

Substrate binding to the APC/C occurs between CDH1 and DOC1

To understand how substrates are recruited to the APC/C and whether DOC1 has a direct role in this process, we mapped the location of a substrate protein on the APC/C by EM and 3D reconstruction. We used human APC/C^{CDH1} for this analysis because we were able to generate sufficient amounts of human CDH1 (His6-HA-CDH1), but not of yeast coactivator proteins, for these experiments. To evaluate which substrate binds to APC/C^{CDH1} stably enough to allow EM mapping experiments, we reconstituted and purified APC/C^{CDH1} bound to either budding yeast Hsl1$_{667–872}$, human sororin or human securin and measured, by immunoblotting over a time course of 6 h, how much substrate remained bound to APC/C^{CDH1}. Many sororin and securin molecules dissociated from APC/C^{CDH1} during the 6-h time course, whereas the majority of Hsl1 remained associated (**Fig. 7a**,**b**), consistent with the previous observation that Hsl1 binds to APC/C particularly tightly[20,29]. These experiments also confirmed that the interaction between APC/C and CDH1 is stabilized by the presence of Hsl1 (refs. 29,30).

We therefore performed all subsequent experiments with the Hsl1$_{667–872}$ fragment. We used a td2-tagged version of Hsl1 (His6-Flag-td2-Hsl1$_{667–872}$) for these experiments, hoping that the td2 domain might help in the subsequent visualization of the substrate in the 3D structure. To ascertain that this protein binds as a bona fide substrate, we isolated APC/C on CDC27 antibody-conjugated Sepharose beads and incubated these with either wild-type Hsl1 or a mutant in which the D box and the KEN box were mutated[31] in either the absence or the presence of CDH1. Unbound CDH1 and Hsl1 were removed by washing the beads, and APC/C was subsequently eluted from the antibody beads by an excess of antigenic CDC27 peptide. SDS-PAGE and silver staining confirmed that only the wild-type fragment of Hsl1 could efficiently bind to the APC/C, and that this interaction was greatly increased by the presence of CDH1 (**Fig. 7c**). Furthermore, incubation of APC/C$^{CDH1–Hsl1}$ complexes with E1, UBCH10 and ubiquitin resulted in the ubiquitylation of Hsl1, further indicating that Hsl1 associated with APC/C^{CDH1} as a functional substrate (**Fig. 7d**). Because substrates have to be turned over rapidly *in vivo*, it was surprising to find that substrates bind to the APC/C relatively stably. This observation raises the interesting possibility that, *in vivo*, additional factors might promote substrate release from the APC/C.

To obtain complexes composed of APC/C, CDH1 and substrate in a 1:1:1 stoichiometry, we further re-isolated proteins bound to Hsl1 by immunoprecipitation using antibodies to Flag, again followed by peptide elution (**Fig. 7c**, last lane). The resulting APC/C$^{CDH1–Hsl1}$ complexes were further purified by glycerol density-gradient centrifugation using the GraFix method[32] and analyzed by cryo-negative

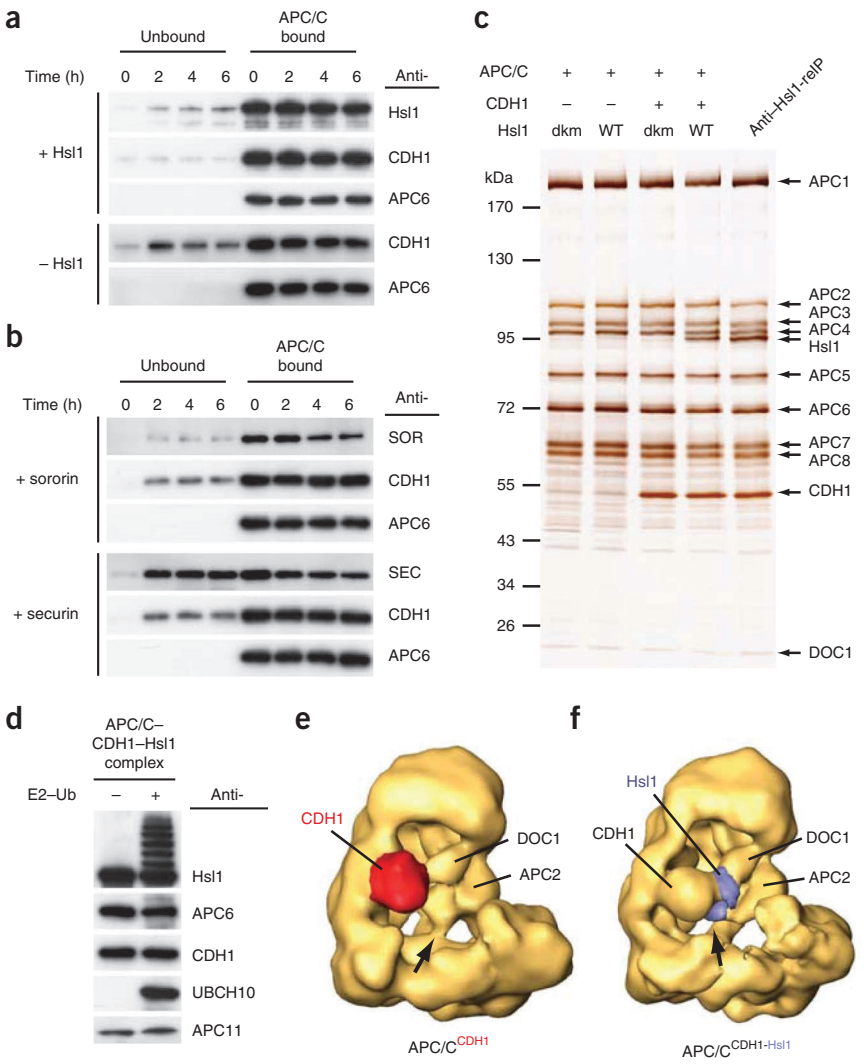

Figure 7 *In vitro* reconstitution of human APC/C bound to a substrate molecule. (**a**) Off-rate determination of Hsl1 and/or CDH1. (**b**) Reconstituted APC/C^{CDH1} complexes bound to either sororin or securin were subjected to off-rate experiments as described in **a**. (**c**) Human APC/C incubated with wild-type (WT) or D box–KEN box mutant (dkm) form of His-Flag-td2-Hsl1$_{667–872}$ in absence or presence of purified CDH1. Re-immunoprecipitation experiments were used to purify stoichiometric APC/C$^{CDH1–Hsl1}$ complexes. (**d**) APC/C$^{CDH1–Hsl1}$ incubated with pre-formed UBCH10–ubiquitin complexes results in formation of Hsl1–ubiquitin conjugates. (**e**) 3D model of human APC/C bound to its coactivator protein CDH1 (red). In the APC/C^{CDH1} structure, the APC2–APC11 module contacts the platform domain (arrow). (**f**) 3D model of human APC/C$^{CDH1–Hsl1}$. The density attributed to the Hsl1 substrate molecule (blue) is intercalated between CDH1 and DOC1. In the APC/C$^{CDH1–Hsl1}$ structure, the contact between APC2–APC11 and the platform is resolved to form a new connection (blue) to the coactivator protein (arrow).

staining EM. The difference map calculated for the structures of APC/C^{CDH1} (ref. 10 and **Fig. 7e**) and APC/C$^{CDH1–Hsl1}$ revealed one prominent extra density in substrate-bound APC/C (**Fig. 7f**). This density was intercalated between the densities that we had identified as CDH1 and DOC1. A second extra density was present near the platform domain, but this density disappeared when the threshold for surface rendering was increased, whereas the prominent density between CDH1 and DOC1 remained (**Supplementary Fig. 4**). The two densities might represent two domains of His6-Flag-td2-Hsl1$_{667–872}$ that are connected by a linker region that we were unable to visualize. Because Hsl1 is known to bind to Cdh1 directly in a manner dependent on the D box and KEN box[31], we suspect that the density near CDH1 and DOC1 represents Hsl1$_{667–872}$, whereas the density near the platform domain may represent the td2 tag, whose position might be more flexible and which therefore might become invisible at increased surface rendering thresholds.

We also noticed that a contact that normally exists between APC2 and a subunit in the platform domain (indicated by a short arrow in **Fig. 7e**) is absent in APC/C$^{CDH1–Hsl1}$ (**Fig. 7e**,**f** and **Supplementary Fig. 5**). Instead, in APC/C$^{CDH1–Hsl1}$, APC2 appears to contact CDH1 directly, in close proximity to where CDH1 contacts the substrate density. These data are consistent with the possibility that the substrate protein forms several contacts on the APC/C, possibly with CDH1 and DOC1, and that substrate binding induces conformational changes in APC2 and/or APC11.

DISCUSSION

Even though the APC/C is essential for cell division, it remains poorly understood how this complex recognizes and ubiquitylates specific substrate proteins, how these processes are controlled in time, and why, in contrast to other ubiquitin ligases, the APC/C comprises at least 13 different subunits. Because structural information will be important for answering these questions, we have used biochemical and EM approaches to identify how the processivity factor Doc1 and a substrate protein interact with the APC/C. Our results also show, that the structure of the APC/C is largely conserved between budding yeast and vertebrates, as well as how two APC/C particles interact to form a 36S dimer.

Although our structural analysis of yeast APC/C revealed many similarities with the structure of human APC/C, there are also important differences. The most notable one is the lack of a density in the arc lamp domain, which results in a reduced height (by 15%) for this domain in yeast APC/C (**Fig. 8** and **Supplementary Fig. 3e**). Because the arc lamp domain is predominantly composed of TPR subunits, it is possible that the density only found in vertebrate APC/C is formed by Apc7, a TPR subunit thus far identified only in higher eukaryotes.

A second peculiarity of budding yeast APC/C is its ability to form dimers[12,23,33], which are the predominant form in yeast whole-cell extracts[23] and which therefore might also exist *in vivo*. This notion is further supported by the fact that we were able to obtain a defined 3D structure of APC/C dimers, which would not be possible if the dimers were formed by nonspecific aggregation of monomers. Our 3D structure reveals that two APC/C monomers interact via multiple discrete contacts involving Cdc27, Cdc16, Apc1 and possibly Apc2. Because these contacts are located on the back side of the arc lamp and the platform domains, the substrate-binding sites within the dimer face

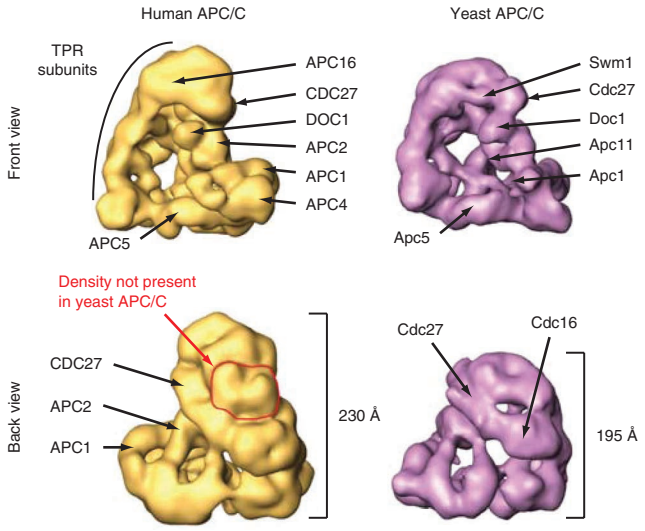

Figure 8 Topological comparison of human and budding yeast APC/C. Human and yeast APC/C models are shown in either front or back view orientation at a resolution of ~25 Å. The positions of mapped subunits are indicated. Note that human APC/C carries a marked extra mass within the TPR-rich arc lamp domain, which might represent a subunit specific for vertebrate APC/C, such as Apc7.

opposite directions. This observation suggests that each monomer within the APC/C dimer can mediate ubiquitylation reactions independent of its dimerization partner. Understanding the functional relevance of APC/C dimerization, and whether such dimers also exist *in vivo*, will therefore require further investigation.

By combining EM structure determination with the deletion or tagging of different subunits, we have identified the position of seven subunits in yeast APC/C. For four of these, we have also mapped the position of their orthologs in human or *Xenopus* APC/C[9,10] (**Supplementary Table 4**). Notably, for all four of these subunits we found that their positions corresponded to each other in the yeast and vertebrate 3D structures. This observation, and the finding that the 3D structures of yeast and human APC/C are similar, makes it possible for the first time to draw an almost complete 3D map of the locations of APC/C subunits (**Fig. 8**). This topographic map is largely consistent with previous biochemical and genetic data[13–15] and indicates that the platform domain is composed of Apc1, Apc4 and Apc5, and the arc lamp domain of Cdc27, Apc16, Swm1, Cdc16, Cdc26, Cdc23 and (in vertebrates) Apc7. Notably, a third, small domain, composed of Apc2, Apc11 and Doc1, is located between the platform and the arc lamp. Because Apc11 is known to recruit E2 enzymes, which transfer ubiquitin residues to substrates[1], we propose to call this domain the "catalytic core."

It is well established that Doc1 is required for efficient substrate recruitment to the APC/C and for processive substrate ubiquitylation[16,17,20], but how Doc1 performs these functions and how Doc1 itself interacts with the APC/C are poorly understood. In cross-linking experiments, we identified Cdc27, Cdc16 and Apc1 as binding partners of Doc1. These results are consistent with our previous observation that Doc1 binds to Cdc27 *in vitro*[5] and with our EM data, which place Doc1 above Apc1, to the right of Cdc16 and below Cdc27 (**Fig. 8**). Furthermore, it has been previously shown that the Doc1 residues Lys129 and Arg130 are required for efficient binding of Doc1 to the APC/C (ref. 20; note that in this study these residues were referred to as Lys162 and Arg163 because the 283-residue version of Doc1 was used). This observation, combined with our finding that Lys129 predominantly cross-links to Cdc16 and the neighboring residue Ser128 predominantly to Apc1, indicate that the interaction of Doc1 with Cdc16 and Apc1 is required for efficient binding of Doc1 to the APC/C. Because genetic experiments had shown that Apc2 is required for recruitment of Doc1 to yeast APC/C[15], it was unexpected that no Doc1–Apc2 cross-link products were obtained, but our EM data reveal that Doc1 is indeed located next to Apc2 and Apc11. It is possible that we were unable to detect Doc1-Apc2 interactions because we did not insert tmd(Phe) into Doc1 residues that contact Apc2. Notably, we observed that two Doc1 residues (Ser128 and Lys129) could each cross-link to two APC/C subunits, Cdc16 and Apc1 (**Supplementary Table 2**), implying that either Ser128 and Lys129 are located directly at the interface of Cdc16 and Apc1, or Doc1 is able to interact with the APC/C in two different ways. This observation raises the interesting possibility that Doc1 could adopt two different conformations on the APC/C and that this ability might be required for Doc1's role in processive substrate ubiquitylation.

How might Doc1 confer processivity to APC/C-mediated ubiquitylation reactions? Our observation that substrate protein is located directly in between DOC1 and CDH1 strongly implies that DOC1 directly interacts with the substrate, as was previously shown to be the case for CDH1 (ref. 28). We therefore propose that Doc1 mediates processive substrate ubiquitylation reactions by forming part of a bipartite substrate receptor on the APC/C, composed of Doc1's ligand binding region[4,5,20] and the WD40 propeller domain of the coactivator protein[28]. This hypothesis is also supported by the previous observation that mutation of the D box in APC/C substrates and deletion of Doc1 reduce substrate ubiquitylation in similar and functionally redundant manners[20]. It is also noteworthy that the major substrate density occupies a position that overlaps with the position of MCC subunits (**Supplementary Fig. 5**), which are believed to inhibit the APC/C as a pseudo-substrate[10,34]. The overlap between the positions of substrate and MCC proteins provides further support for the hypothesis that MCC inactivates the APC/C by occupying and/or altering its substrate-binding site.

METHODS

Methods and any associated references are available in the online version of the paper at http://www.nature.com/nsmb/.

Accession numbers. Electron Microscopy Database: yeast APC/C monomer, EMD-1820; yeast APC/C dimer, EMD-1822; human APC/$C^{CDH1–Hsl1}$, EMD-1821.

Note: Supplementary information is available on the Nature Structural & Molecular Biology website.

ACKNOWLEDGMENTS

We are grateful to I. Häcker (Max Planck Institute for Biophysical Chemistry, Göttingen) and M. Madalinski (IMP, Vienna) for technical assistance; J. Barrett (Zentrum für Molekulare Biologie, Heidelberg), J. Brunner (Eidgenössische Technische Hochschule Zürich), D. Finley (Harvard Medical School, Boston), U. Hoya (Friedrich-Alexander-Universität, Erlangen), D. Morgan (University of California, San Francisco), K. Nasmyth (University of Oxford), M. Solomon (Yale University) and W. Zachariae (Max Planck Institute of Molecular Cell Biology and Genetics, Dresden) for kindly providing yeast strains and reagents; and J. Barrett, J. Brunner and B. Martoglio (Eidgenössische Technische Hochschule Zürich) for advice on photo-cross-linking. Research in the laboratory of H.S. was supported by grants from the Federal Ministry of Education and Research, Germany, and from the Sixth Framework Programme of the European Union via the Integrated Project 3DRepertoire. Research in the laboratory of J.-M.P. is supported by Boehringer Ingelheim, the Vienna Spots of Excellence Programme and the Austrian Science Fund.

AUTHOR CONTRIBUTIONS
H.S. and J.-M.P. planned and supervised the project. B.A.B., G.P., C.K. and F.H. designed the experiments. B.A.B. performed most of the photo-cross-linking and biochemical experiments on yeast APC/C. G.P. performed the experiments on substrate bound APC/C. M.G. and C.K. generated yeast strains and performed growth assays and yeast APC/C purifications. F.H. performed antibody labeling on human APC/C. P.D. performed EM. H.S. calculated and analyzed the 3D EM structures. B.A.B., G.P. and J.-M.P. wrote the paper.

COMPETING FINANCIAL INTERESTS
The authors declare no competing financial interests.

Published online at http://www.nature.com/nsmb/.
Reprints and permissions information is available online at http://npg.nature.com/reprintsandpermissions/.

1. Peters, J.M. The anaphase promoting complex/cyclosome: a machine designed to destroy. *Nat. Rev. Mol. Cell Biol.* **7**, 644–656 (2006).
2. Matyskiela, M.E., Rodrigo-Brenni, M.C. & Morgan, D.O. Mechanisms of ubiquitin transfer by the anaphase-promoting complex. *J. Biol.* **8**, 92 (2009).
3. Musacchio, A. & Salmon, E.D. The spindle-assembly checkpoint in space and time. *Nat. Rev. Mol. Cell Biol.* **8**, 379–393 (2007).
4. Au, S.W., Leng, X., Harper, J.W. & Barford, D. Implications for the ubiquitination reaction of the anaphase-promoting complex from the crystal structure of the Doc1/Apc10 subunit. *J. Mol. Biol.* **316**, 955–968 (2002).
5. Wendt, K.S. *et al.* Crystal structure of the APC10/DOC1 subunit of the human anaphase-promoting complex. *Nat. Struct. Biol.* **8**, 784–788 (2001).
6. Wang, J., Dye, B.T., Rajashankar, K.R., Kurinov, I. & Schulman, B.A. Insights into anaphase promoting complex TPR subdomain assembly from a CDC26–APC6 structure. *Nat. Struct. Mol. Biol.* **16**, 987–989 (2009).
7. Zhang, Z. *et al.* Molecular structure of the N-terminal domain of the APC/C subunit Cdc27 reveals a homo-dimeric tetratricopeptide repeat architecture. *J. Mol. Biol.* **397**, 1316–1328 (2010).
8. Han, D., Kim, K., Kim, Y., Kang, Y. & Lee, J.Y. Crystal structure of the N-terminal domain of anaphase-promoting complex subunit 7. *J. Biol. Chem.* **284**, 15137–15146 (2009).
9. Dube, P. *et al.* Localization of the coactivator Cdh1 and the cullin subunit Apc2 in a cryo-electron microscopy model of vertebrate APC/C. *Mol. Cell* **20**, 867–879 (2005).
10. Herzog, F. *et al.* Structure of the anaphase-promoting complex/cyclosome interacting with a mitotic checkpoint complex. *Science* **323**, 1477–1481 (2009).
11. Ohi, M.D. *et al.* Structural organization of the anaphase-promoting complex bound to the mitotic activator Slp1. *Mol. Cell* **28**, 871–885 (2007).
12. Passmore, L.A. *et al.* Structural analysis of the anaphase-promoting complex reveals multiple active sites and insights into polyubiquitylation. *Mol. Cell* **20**, 855–866 (2005).
13. Vodermaier, H.C., Gieffers, C., Maurer-Stroh, S., Eisenhaber, F. & Peters, J.M. TPR subunits of the anaphase-promoting complex mediate binding to the activator protein CDH1. *Curr. Biol.* **13**, 1459–1468 (2003).
14. Schwickart, M. *et al.* Swm1/Apc13 is an evolutionarily conserved subunit of the anaphase-promoting complex stabilizing the association of Cdc16 and Cdc27. *Mol. Cell. Biol.* **24**, 3562–3576 (2004).
15. Thornton, B.R. *et al.* An architectural map of the anaphase-promoting complex. *Genes Dev.* **20**, 449–460 (2006).
16. Passmore, L.A. *et al.* Doc1 mediates the activity of the anaphase-promoting complex by contributing to substrate recognition. *EMBO J.* **22**, 786–796 (2003).
17. Carroll, C.W. & Morgan, D.O. The Doc1 subunit is a processivity factor for the anaphase-promoting complex. *Nat. Cell Biol.* **4**, 880–887 (2002).
18. Grossberger, R. *et al.* Characterization of the DOC1/APC10 subunit of the yeast and the human anaphase-promoting complex. *J. Biol. Chem.* **274**, 14500–14507 (1999).
19. Gieffers, C., Schleiffer, A. & Peters, J.M. Cullins and cell cycle control. *Protoplasma* **211**, 20–28 (2000).
20. Carroll, C.W., Enquist-Newman, M. & Morgan, D.O. The APC subunit Doc1 promotes recognition of the substrate destruction box. *Curr. Biol.* **15**, 11–18 (2005).
21. Hwang, L.H. & Murray, A.W. A novel yeast screen for mitotic arrest mutants identifies DOC1, a new gene involved in cyclin proteolysis. *Mol. Biol. Cell* **8**, 1877–1887 (1997).
22. Brunner, J. New photolabeling and crosslinking methods. *Annu. Rev. Biochem.* **62**, 483–514 (1993).
23. Zachariae, W., Shin, T.H., Galova, M., Obermaier, B. & Nasmyth, K. Identification of subunits of the anaphase-promoting complex of *Saccharomyces cerevisiae*. *Science* **274**, 1201–1204 (1996).
24. Campbell, R.E. *et al.* A monomeric red fluorescent protein. *Proc. Natl. Acad. Sci. USA* **99**, 7877–7882 (2002).
25. Häcker, I. *et al.* Localization of Prp8, Brr2, Snu114 and U4/U6 proteins in the yeast tri-snRNP by electron microscopy. *Nat. Struct. Mol. Biol.* **15**, 1206–1212 (2008).
26. Hall, M.C., Torres, M.P., Schroeder, G.K. & Borchers, C.H. Mnd2 and Swm1 are core subunits of the *Saccharomyces cerevisiae* anaphase-promoting complex. *J. Biol. Chem.* **278**, 16698–16705 (2003).
27. Yoon, H.J. *et al.* Proteomics analysis identifies new components of the fission and budding yeast anaphase-promoting complexes. *Curr. Biol.* **12**, 2048–2054 (2002).
28. Kraft, C., Vodermaier, H.C., Maurer-Stroh, S., Eisenhaber, F. & Peters, J.M. The WD40 propeller domain of Cdh1 functions as a destruction box receptor for APC/C substrates. *Mol. Cell* **18**, 543–553 (2005).
29. Matyskiela, M.E. & Morgan, D.O. Analysis of activator-binding sites on the APC/C supports a cooperative substrate-binding mechanism. *Mol. Cell* **34**, 68–80 (2009).
30. Burton, J.L., Tsakraklides, V. & Solomon, M.J. Assembly of an APC-Cdh1-substrate complex is stimulated by engagement of a destruction box. *Mol. Cell* **18**, 533–542 (2005).
31. Burton, J.L. & Solomon, M.J. D box and KEN box motifs in budding yeast Hsl1p are required for APC-mediated degradation and direct binding to Cdc20p and Cdh1p. *Genes Dev.* **15**, 2381–2395 (2001).
32. Kastner, B. *et al.* GraFix: sample preparation for single-particle electron cryomicroscopy. *Nat. Methods* **5**, 53–55 (2008).
33. Passmore, L.A. & Barford, D. Coactivator functions in a stoichiometric complex with anaphase-promoting complex/cyclosome to mediate substrate recognition. *EMBO Rep.* **6**, 873–878 (2005).
34. Burton, J.L. & Solomon, M.J. Mad3p, a pseudosubstrate inhibitor of APCCdc20 in the spindle assembly checkpoint. *Genes Dev.* **21**, 655–667 (2007).
35. Sheff, M.A. & Thorn, K.S. Optimized cassettes for fluorescent protein tagging in *Saccharomyces cerevisiae*. *Yeast* **21**, 661–670 (2004).

ONLINE METHODS

Strains and plasmids. Yeast genetic manipulations were carried out using standard protocols. For untagged Doc1 constructs in pME vectors, pME34 (ref. 20) was used and the original STOP codon of the open reading frame (ORF) was kept. To introduce *DOC1*, including its endogenous promoter, into pRS316, the *DOC1* ORF plus 154 bases upstream of the translation start and 158 bases downstream were amplified from yeast genomic DNA and cloned into pRS316 via EcoRI sites. Amber (TAG) and ochre (TAA) STOP codons as well as alanine and phenylalanine mutations were generated using the QuikChange method (Stratagene). For tagging of APC/C subunits with tdimer2, pKT146 was used[35]. Detailed information about N-terminal tagging of Doc1 with tdimer2, as well as a list of yeast strains (**Supplementary Table 5**) used, are provided in the **Supplementary Methods**.

APC/C purification. Yeast cells were grown in YPD rich medium (1% (w/v) yeast extract, 2% (w/v) peptone, 2% (w/v) glucose). At OD_{600}, cells were harvested by centrifugation and washed with EM lysis buffer (20 mM HEPES-KOH, pH 8.0, 200 mM KCl, 10% (v/v) glycerol, 1.5 mM $MgCl_2$). Yeast extracts were prepared by bead beating for cross-linking experiments. For EM experiments, frozen cells were ground in a mortar grinder (RM100, Retsch), whereas a freezer mill (SPEX Freezer/Mill 6770, 6780) was used for all other applications. APC/C isolation by tandem affinity purification was carried out as described[16,36]. For each EM experiment, cells from 40 liters of yeast culture were lysed in the presence of 0.03% (w/v) octyl-β-D-glucopyranoside, and APC/C was eluted with 3 mM EGTA. 500 µl APC/C eluate was loaded onto a 10–40% (v/v) glycerol density gradient (20 mM HEPES-KOH, pH 7.9, 150 mM NaCl, 2 mM $MgCl_2$, 0.05% (w/v) octyl-β-D-glucopyranoside) containing 0.05–0.2% (v/v) glutaraldehyde[32] and centrifuged at 37,000 r.p.m. (140,601*g*) for 14 h at 4 °C in a Beckman SW60Ti rotor. APC/C peak fractions were used for subsequent EM experiments.

Photo-cross-linking. TNT rabbit reticulocyte lysates were used to incorporate photoactivatable cross-linkers into the Doc1 protein. Reactions were supplemented with 1 mM magnesium acetate and 1.6 µl (tmd)Phe-tRNA (see below) per 50 µl reaction. Photo-cross-linking experiments were carried out with freshly prepared yeast cell extracts (50 mM Tris-HCl, pH 8, 150 mM NaCl, 10% (v/v) glycerol, 0.1% (v/v) NP40). Samples containing photo-cross-linkers were light-protected in all steps. APC/C was bound to IgG–Sepharose beads by incubating extract and Sepharose (Bio-Rad) (1–2 mg protein per 5 µl beads) for 60–90 min at 4 °C. Beads were washed with buffer used for cell lysis before addition of TNT rabbit reticulocyte lysate containing *in vitro*–translated Doc1 versions carrying a photo-cross-linker at distinct sites. Samples were incubated at room temperature for 20 min and subsequently washed 3–4 times with lysis buffer. For photo-cross-linking, samples with lids opened were kept in a Thermomixer (Eppendorf) (1,300 r.p.m., 9 °C) and exposed to a black-ray long-UV lamp (B-100AP, 100 W, UVP) with a wavelength of 360 nm at a distance of 10 cm for 5–8 min. APC/C was eluted by the addition of SDS sample buffer.

***In vitro* reconstitution of APC/C bound to human CDH1 and substrates.** Cell extracts were prepared by lysis of frozen log-phase HeLa cells in extract buffer (20 mM Tris-HCl, pH 7.5, 150 mM NaCl, 2 mM EDTA, 10% (v/v) glycerol, 0.05% (v/v) Tween-20) using a Dounce homogenizer followed by centrifugation. APC/C was immunoprecipitated (IP) from the soluble fraction by incubation with CDC27 antibodies[37] cross-linked to Affi-prep protein A beads (Bio-Rad) for 1 h at 4 °C. Beads were washed four times with at least 20 bead volumes of wash buffer (20 mM Tris-HCl, pH 7.5, 150 mM NaCl, 10% (v/v) glycerol, 0.05% (v/v) Tween-20) for 3 min at 4 °C. To reconstitute coactivator- and/or substrate-bound APC/C complexes *in vitro*, APC/C-bound CDC27 beads were resuspended in binding buffer (20 mM Tris-HCl, pH 7.5, 150 mM NaCl, 0.05% (v/v) Tween-20, 4 mg ml^{-1} BSA) supplemented with 3.5 µM recombinant human CDH1 and/or 150 nM recombinant wild-type or mutant (D box and KEN box mutated) His-Flag-td2-$Hsl1_{667–872}$, sororin-td2-Flag-His or securin-Flag-His. After a 1-h incubation at 4 °C, the excess of recombinant proteins was removed by washing the beads four times with at least 20 bead volumes of wash buffer for 3 min at 4 °C, and APC/C complexes were recovered by elution with antigenic peptides. $APC/C^{CDH1–Hsl1}$ complexes were enriched by re-immunoprecipitation (re-IP) experiments using ANTI-FLAG M2 Agarose (Sigma) and recovered by elution with antigenic peptides. For EM experiments, APC/C specimens were subjected to GraFix[32] to further purify and stabilize the complexes. Human recombinant CDH1 was expressed in baculovirus-infected Sf9 insect cells. Recombinant His-Flag-td2-$Hsl1_{667–872}$, sororin-td2-Flag-His and securin-Flag-His substrate proteins were expressed and purified from *Escherichia coli* BL21(DE3) or Rosetta(DE3). The $Hsl1_{667–872}$ sequence was derived from *S. cerevisiae* and sororin and securin from *Homo sapiens*. To demonstrate activity of *in vitro*–reconstituted $APC/C^{CDH1–Hsl1}$ complexes, 50 µl eluate was incubated with 5 µl reaction mix containing preloaded UBCH10–monoubiquitin, E1, ATP and DTT for 1 h at 4 °C.

Off-rate experiments. *In vitro*–reconstituted substrate-bound APC/C^{CDH1} on 25 µl CDC27 antibody–conjugated beads was resuspended in 50 µl wash buffer and incubated on a orbital rotator for 1 min (time point 0), 2, 4 and 6 h. CDC27 antibody–conjugated beads were spun down, wash buffer was saved (unbound fraction) for subsequent SDS-PAGE analysis, and APC/C complexes were recovered by elution with 50 µl antigenic peptides. APC/C-bound and unbound fractions were analyzed by western blotting.

36. Passmore, L.A., Barford, D. & Harper, J.W. Purification and assay of the budding yeast anaphase-promoting complex. *Methods Enzymol.* **398**, 195–219 (2005).
37. Gieffers, C., Dube, P., Harris, J.R., Stark, H. & Peters, J.M. Three-dimensional structure of the anaphase-promoting complex. *Mol. Cell* **7**, 907–913 (2001).

doi:10.1038/nsmb.1979